

## MODELLING OF THE TORSION AND COMBINED ELONGATION–TORSION TESTS OF HYPERELASTIC CYLINDERS

A. Poživilová\*, J. Plešek†

**Summary:** *Stress effects in an incompressible hyperelastic cylindrical specimen are specified for the torsion test and combined elongation–torsion tests. The twisting couple and the axial force are specified for Hencky’s material model and are compared with the classic models. The results include the well-known Poynting effect.*

### 1. Introduction

The validity of a particular hyperelastic theory is usually tested by comparison of predictions of material responses of the rubber specimens with experimental results. Some simple deformation modes are quite suitable for this comparison. The elongation or compression load–stretch characteristics are classic experiments used for the assessment of particular material model since the abundant experimental works of Treloar [16]. Later, the experiments on natural rubber carried out by Rivlin and Saunders [14] became very popular not only for verifications of different material models but also for the identification of material parameters.

Rivlin and Saunders in the aforementioned article published data from the extension test, the compression test, the pure shear test, and from the biaxial tests with constant strain invariants, all of them carried out on the specimens cut from one piece of a rubber band. Further, they presented experimental results of the torsion test and combined extension–torsion test on a cylindrical specimens. Since then, the results of these experiments served for comparison and verification of different material models of hyperelastic material.

In this work, we pay attention to the response of rubber in torsion test and combined elongation–torsion test of cylindrical specimens.

It should be stressed that in the course of torsion, the cylindrical specimens must be loaded by axial force to fix the axial length. This effect is known as Poynting effect.

---

\*Ing. Alena Poživilová, Ph.D.: Institute of Thermomechanics, Academy of Sciences of the Czech Republic; Dolejšková 5; 182 00 Praha 8; tel. +420 266 053 792; fax: +420 285 584 695; email: alena@it.cas.cz

†Ing. Jiří Plešek, CSc.: Institute of Thermomechanics, Academy of Sciences of the Czech Republic; Dolejšková 5; 182 00 Praha 8; tel. +420 266 053 213; fax: +420 285 584 695; email: plesek@it.cas.cz

Poynting showed in [10] and [11] that a wire when twisted lengthens by an amount proportional to the square of the angle of twist. This result is expected from the analysis of strain under finite pure shear, when second-order effects are supposed.

The analytical response of the Mooney–Rivlin material model [6] is linear and can be found in [14]. Later, Ogden and Chadwick in their paper [8] presented the analytical solution for a three-term Ogden’s material model [7].

The Hencky material model, which is based on the linear relation between the logarithmic strain and conjugate stress, was presented in Anand [1]. In this paper, Anand showed a good agreement of the proposed theory with experiment for moderately large deformation in uniaxial strain, simple tension and compression and pure shear. Later on, Anand [2] published the responses of the Hencky’s material model for the twisting moment and axial force loadings in simple torsion and combined elongation–torsion tests and showed that they are in a good agreement with data from the classic experiments of Rivlin and Saunders.

However, different results can be found in a more recent article by Bruhns, Xiao and Meyers, [3]. This discrepancy lead to the derivation presented here because the exact solution was necessary for fitting the experimental data by Sedlan [15], [4].

In the first part, the kinematics of deformation is sketched. Stress conditions in the twisted cylinder and in the cylinder which underwent elongation and twisting are given. Subsequently, the relations for the magnitude of the twisting couple and axial force are derived. These results are assessed in Section 7.

## 2. Kinematics of the deformation

Let  $(R, \Theta, Z)$  be the cylindrical coordinates in reference configuration and their counterpart in the current configuration are  $(r, \theta, z)$ .  $R$  is the radius,  $\Theta$  represents the angle oriented counterclockwise with respect to the Cartesian  $x$ -axis in the  $xy$ -plane and  $Z$  is parallel to the axis of the cylinder, see Fig. 1.

$$\begin{aligned} r &= \lambda^{-1/2} R \\ \theta &= \Theta + \tau \lambda Z \\ z &= \lambda Z \end{aligned} \tag{1}$$

where  $\tau$  represents an angle per deformed length and describes the relative distortion of the top and bottom planes of the body per distance of the planes and is called twist.

The deformation gradient related to the Cartesian coordinates takes the form

$$\mathbf{F} = \begin{bmatrix} \cos \theta & -\sin \theta & 0 \\ \sin \theta & \cos \theta & 0 \\ 0 & 0 & 1 \end{bmatrix} \begin{bmatrix} \lambda^{-1/2} & 0 & 0 \\ 0 & \lambda^{-1/2} & \tau R \lambda^{1/2} \\ 0 & 0 & \lambda \end{bmatrix} \begin{bmatrix} \cos \Theta & \sin \Theta & 0 \\ -\sin \Theta & \cos \Theta & 0 \\ 0 & 0 & 1 \end{bmatrix} \tag{2}$$

The Cauchy–Green deformation tensor  $\mathbf{C}$  related to the cylindrical coordinates  $(R, \Theta, Z)$

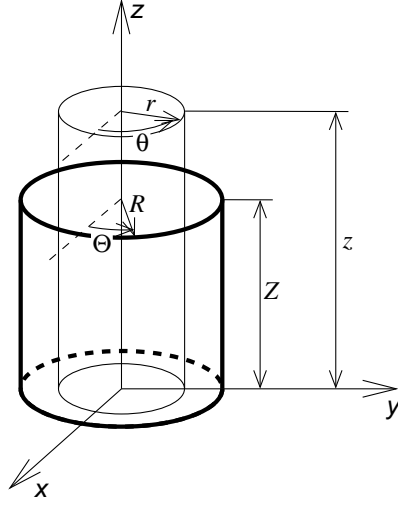


Figure 1: Extension and torsion of a cylinder, the cylindrical coordinates

is

$$\tilde{\mathbf{C}} = \begin{bmatrix} \lambda^{-1} & 0 & 0 \\ 0 & \lambda^{-1} & \tau R \\ 0 & \tau R & \lambda (\tau R)^2 + \lambda^2 \end{bmatrix} \quad (3)$$

Denoting

$$B = \lambda^{-1} + \lambda^2 + \lambda (\tau R)^2 \quad (4)$$

we can rewrite the principal stretches as

$$\lambda_1 = \lambda^{-1/2} \quad \lambda_2 = \sqrt{\frac{B + \sqrt{B^2 - 4\lambda}}{2}} \quad \lambda_3 = \sqrt{\frac{B - \sqrt{B^2 - 4\lambda}}{2}} \quad (5)$$

The logarithmic stretch tensor is

$$\ln \mathbf{U} = \begin{bmatrix} -\frac{1}{2} \ln \lambda & 0 & 0 \\ 0 & \frac{\ln \lambda_2 (\lambda^{-1} - \lambda_3^2) + \ln \lambda_3 (\lambda_2^2 - \lambda^{-1})}{\lambda_2^2 - \lambda_3^2} & \tau R \frac{\ln \lambda_2 - \ln \lambda_3}{\lambda_2^2 - \lambda_3^2} \\ 0 & \tau R \frac{\ln \lambda_2 - \ln \lambda_3}{\lambda_2^2 - \lambda_3^2} & \frac{\ln \lambda_2 (\lambda_2^2 - \lambda^{-1}) + \ln \lambda_3 (\lambda^{-1} - \lambda_3^2)}{\lambda_2^2 - \lambda_3^2} \end{bmatrix} \quad (6)$$

### 3. Stresses

The stress conjugate to the logarithmic strain tensor is the logarithmic stress, see [5]. For isotropic materials, the stress obtained from the constitutive relation reduces to the

back rotated Kirchhoff stress  $\mathbf{T}$ . For more details, see [12], [13] or [9]. The Hencky material model is based on the linear relation between the logarithmic strain and the logarithmic stress (see [1], [12])

$$\mathbf{T} = \Lambda \operatorname{tr}(\ln \mathbf{U}) + 2\mu \ln \mathbf{U} \quad (7)$$

where  $\Lambda$  and  $\mu$  are Lamé constants. Because the deformation of any incompressible material is volume preserving, the trace of the logarithmic strain tensor is zero, that is  $\operatorname{tr}(\ln \mathbf{U}) = 0$ . On the other hand, the stress components are not fully determined by deformation as the hydrostatic part of the stress tensor must be determined from the boundary conditions.

Substituting the logarithmic strain tensor (6) into (7), we get the distortional part of the back rotated Kirchhoff stress tensor. The relation between the distortional part of the back rotated Kirchhoff stress and distortional part of the Cauchy stress tensor is

$$\boldsymbol{\sigma}_d = J^{-1} \mathbf{R} \mathbf{T}_d \mathbf{R}^T \quad (8)$$

where  $J = \det \mathbf{F}$  is the Jacobian of deformation, which is equal to one for incompressible materials and  $\mathbf{R}$  is the rotation tensor obtained from the polar decomposition of the deformation gradient.

The components of the Cauchy stress tensor in the cylindrical coordinate system  $(r, \theta, z)$  are

$$\begin{aligned} \sigma_{rr} &= -\mu \ln \lambda = -2\mu (\ln \lambda_2 + \ln \lambda_3) - p \\ \sigma_{\theta\theta} &= 2\mu \frac{\ln \lambda_2 (\lambda_2^2 - \lambda_3^2) + \ln \lambda_3 (\lambda_2^2 - \lambda_3^2)}{\lambda_2^2 - \lambda_3^2} - p \\ \sigma_{zz} &= 2\mu \frac{\ln \lambda_2 (\lambda_2^2 - \lambda_3^2) + \ln \lambda_3 (\lambda_2^2 - \lambda_3^2)}{\lambda_2^2 - \lambda_3^2} - p \\ \sigma_{\theta z} &= 2\mu \tau R \lambda^{3/2} \frac{\ln \lambda_2 - \ln \lambda_3}{\lambda_2^2 - \lambda_3^2} = 2\mu \tau r \lambda^2 \frac{\ln \lambda_2 - \ln \lambda_3}{\lambda_2^2 - \lambda_3^2} \\ \sigma_{z\theta} &= \sigma_{\theta z} \\ \sigma_{zr} &= \sigma_{rz} = 0 \\ \sigma_{r\theta} &= \sigma_{\theta r} = 0 \end{aligned} \quad (9)$$

The equation of equilibrium corresponding to the stress field in the cylinder takes the form

$$\frac{\partial \sigma_{rr}}{\partial r} + \frac{\sigma_{rr} - \sigma_{\theta\theta}}{r} = 0 \quad (10)$$

where  $\sigma_{rr}$ ,  $\sigma_{\theta\theta}$  and  $\sigma_{zz}$  denotes the Cauchy stress components in radial, tangential and axial directions, respectively, and  $\sigma_{\theta z}$  is the shear component of the stress field.

#### 4. Load-deformation characteristics

Expressions for the twisting couple  $M$  and the axial force  $N$  required to compare experimental data with prediction of the model can be obtained in the explicit form.

We suppose the cylinder with the original radius of  $R_1$ . The force in the axial direction causing the elongation is then

$$N = 2\pi \int_0^{R_1} \frac{r^2}{R} \sigma_{zz} dR = 2\pi \int_0^{R_1 \lambda^{-1/2}} \sigma_{zz} r dr \quad (11)$$

The torsional couple  $M$  [Nm] is

$$M = 2\pi \int_0^{R_1} \frac{r^3}{R} \sigma_{z\theta} dR = 2\pi \int_0^{R_1 \lambda^{-1/2}} \sigma_{z\theta} r^2 dr \quad (12)$$

It can easily be proved that the equation (11) can be rewritten to the form

$$N = \pi \int_0^{R_1 \lambda^{-1/2}} [(\sigma_{rr} - \sigma_{\theta\theta}) + 2(\sigma_{zz} - \sigma_{rr})] dr \quad (13)$$

This procedure enables the exact integration of relation (11). The results are

$$M = 4\pi\mu\tau^{-3}\lambda^{-3/2} \left[ \ln a (a^2 - a^{-2}) - \frac{a^2 + a^{-2}}{2} - (\lambda^{3/2} + \lambda^{-3/2}) (\ln a)^2 \right]_{\lambda^{3/4}}^{a_r} \quad (14)$$

and

$$N = -3\pi\mu\tau^{-2}\lambda^{-3/2} \left[ \ln a (a^2 - a^{-2}) - \frac{a^2 + a^{-2}}{2} - 2\lambda^{3/2} (\ln a)^2 - \ln \lambda \frac{a^2 + a^{-2}}{4} \right]_{\lambda^{3/4}}^{a_r} \quad (15)$$

where

$$a_r = \frac{1}{2} \left\{ \sqrt{\tau^2 R_1^2 \lambda^{1/2} + (\lambda^{3/2} + \lambda^{-3/2})^2} + \sqrt{\tau^2 R_1^2 \lambda^{1/2} + (\lambda^{3/2} - \lambda^{-3/2})^2} \right\} \quad (16)$$

To illustrate the behaviour of the Hencky model for the biaxial deformation and to compare it with another hyperelastic models we have to put the relations (14) and (15) into dimensionless form. Denote the maximum nominal shear strain at the surface  $\chi = \tau R_1$ , the non-dimensional expressions for  $M^* = \mu^{-1} R_1^{-3} M$  and  $N^* = \mu^{-1} R_1^{-2} N$  are

$$M^* = 4\pi\chi^{-3}\lambda^{-3/2} \left[ \ln a (a^2 - a^{-2}) - \frac{a^2 + a^{-2}}{2} - (\lambda^{3/2} + \lambda^{-3/2}) (\ln a)^2 \right]_{\lambda^{3/4}}^{a_r} \quad (17)$$

and

$$N^* = -3\pi\chi^{-2}\lambda^{-3/2} \left[ \ln a (a^2 - a^{-2}) - \frac{a^2 + a^{-2}}{2} - 2\lambda^{3/2} (\ln a)^2 - \ln \lambda \frac{a^2 + a^{-2}}{4} \right]_{\lambda^{3/4}}^{a_r} \quad (18)$$

$M^*$  as a function of  $\chi$  is illustrated in Fig. 2 for several values of  $\lambda$ . In Fig. 3,  $N^*$  is plotted as a function of  $\chi^2$ , again for several values of  $\lambda$ . In Fig. 2, the origin has been shifted to the right for each successive value of  $\lambda$  so as to avoid congestion.

The special case of combined deformation, when the cylindrical specimen is loaded only by the twisting moment, is obtained setting the axial force (18) equal to zero. This can be solved numerically and the relation of the stretch on the twist is given in Fig. 4.

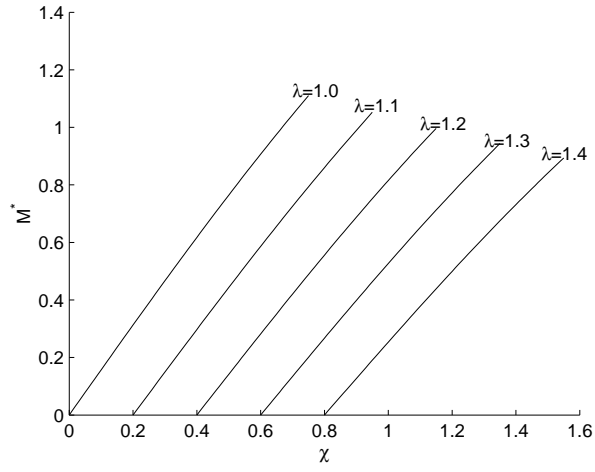


Figure 2: Dependence of  $M^*$  on  $\chi$  for the logarithmic quadratic strain energy function for indicated values of  $\lambda$

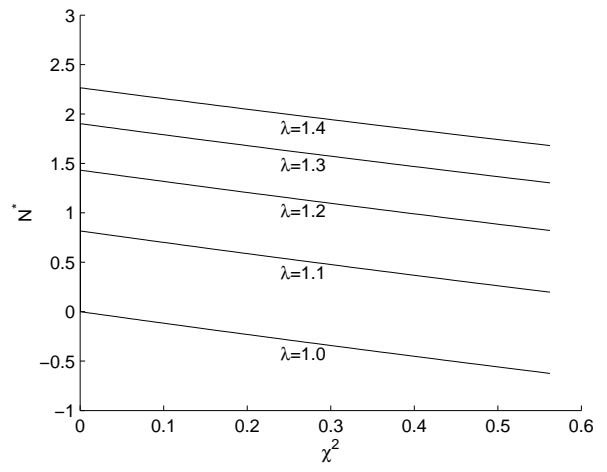


Figure 3: Dependence of  $N^*$  on  $\chi^2$  for the logarithmic quadratic strain energy function for indicated values of  $\lambda$

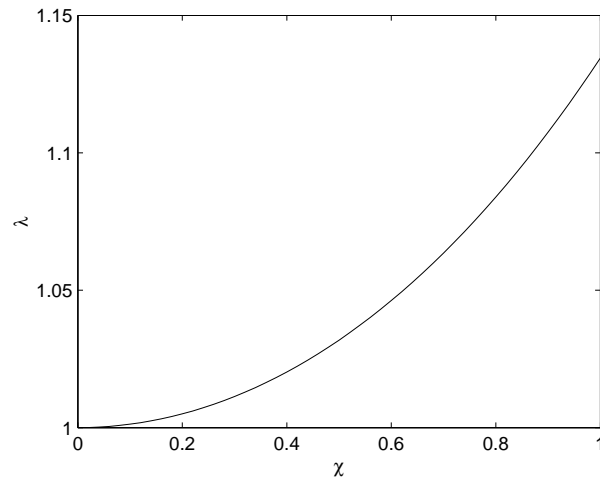


Figure 4: Axial strain  $\lambda$  versus maximum shear strain  $\chi$  for zero axial force.

## 5. Comparison with the standard models

The solution of the biaxial problem for Mooney-Rivlin material model was published in [14]. The relations between  $M^* = \mu^{-1} R_1^{-3} M$  and  $\chi$  is linear

$$M^* = \pi (C_1^* + C_2^* \lambda^{-1}) \chi \quad (19)$$

where

$$C_1^* = C_1 \mu^{-1} \quad \text{and} \quad C_2^* = C_2 \mu^{-1} \quad \text{and} \quad \mu = 2(C_1 - C_2) \quad (20)$$

The relation between  $N^*$  and  $\chi^2$  is also linear

$$N^* = -\frac{\pi}{2} (C_1^* + 2C_2^* \lambda^{-1}) \chi^2 + 2\pi (C_1^* + C_2^* \lambda^{-1}) (\lambda - \lambda^{-2}) \quad (21)$$

The load versus stretch curves for neo-Hookean material model are obtained from the relations for Mooney-Rivlin material model by setting  $C_2 = 0$ . The curves of  $M$  and  $N$  are, of course, also linear in terms of  $\chi$  and  $\chi^2$ , resp.

The analytical solution of the biaxial deformation of a cylindrical specimen for the Ogden material model was published in [8] and can be written as

$$M = 2\pi\tau^{-3} \mu_n \lambda^{1/4\alpha_n - 3/2} \left\{ F(\lambda^{3/4}, a_r, \alpha_n + 2) + F(\lambda^{3/4}, a_r, \alpha_n - 2) - \right. \\ \left. - (\lambda^{3/2} + \lambda^{-3/2}) F(\lambda^{3/4}, a_r, \alpha_n) \right\} \quad (22)$$

where the function  $F$  is

$$F(x, y, \alpha) = \frac{(y^{\alpha/2} - y^{-\alpha/2})^2 - (x^{\alpha/2} - x^{-\alpha/2})^2}{\alpha} \quad \text{with} \quad F(x, y, 0) = 0 \quad (23)$$

The axial force is

$$N = -\pi\tau^{-2} \mu_n \lambda^{1/4\alpha_n - 3/2} \left\{ F(\lambda^{3/4}, a_r, \alpha_n + 2) + 2F(\lambda^{3/4}, a_r, \alpha_n - 2) - \right. \\ \left. - 3\lambda^{3/2} F(\lambda^{3/4}, a_r, \alpha_n) \right\} - \frac{1}{2} \pi R^2 \mu_n \lambda^{-1/2\alpha_n - 1} \quad (24)$$

The dimensionless form of equations (22) and (24) with  $\mu_n^* = \mu^{-1} \mu_n$  and  $\mu = 0.5 \mu_n \alpha_n$  yields

$$M^* = \mu^{-1} R^{-3} M \quad (25)$$

and

$$N^* = \mu^{-1} R^{-2} N \quad (26)$$

The relations for the non-dimensional torsional couple and the non-dimensional axial force are illustrated in Figs. 5 and 6.

## 6. Conclusions

The relations for the axial force and twisting couple in the torsion and combined elongation-torsion tests were derived. It came out, that the expressions found in the older paper by Anand [2] are exact and that Bruhns expressions contain unnecessary approximations.

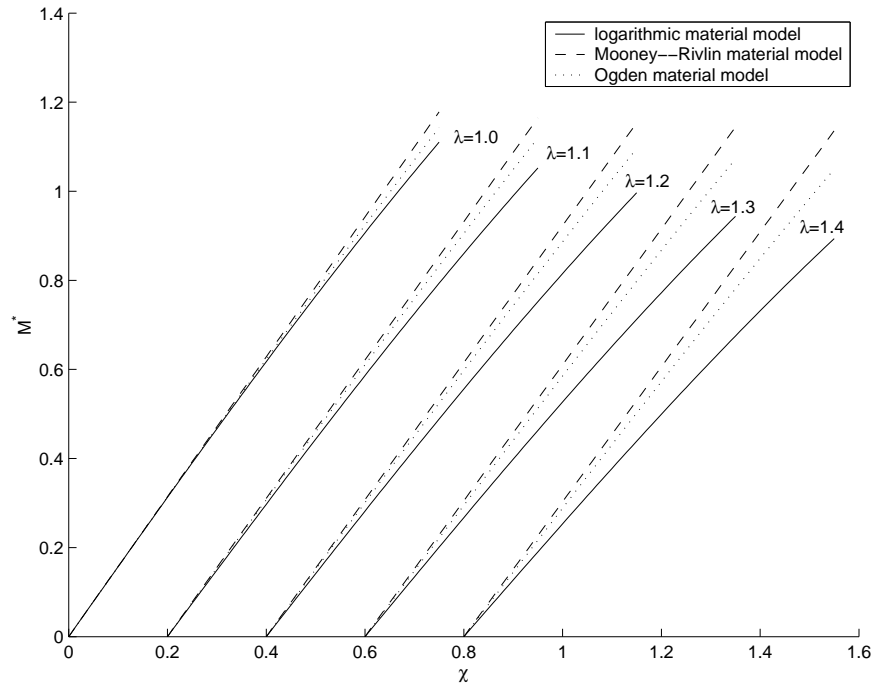


Figure 5: Dependence of the non-dimensional torsional couple  $M^*$  on  $\chi$ . Comparison of different material models.

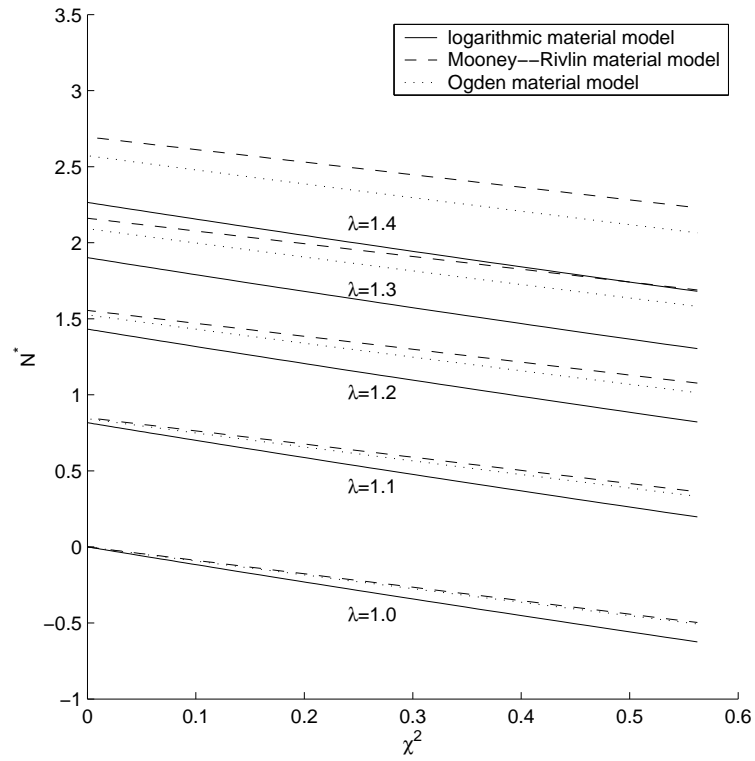


Figure 6: Dependence of the non-dimensional axial force  $N^*$  on  $\chi^2$ . Comparison of different material models.

## 7. Acknowledgements

This work was sponsored by the Grant Agency CR under post-doc project No. 106/03/D038 and the research project No. AVOZ 2076919.

## References

- [1] L. Anand. On Hencky's approximate strain-energy function for moderate deformations. *Journal of Applied Mechanics ASME*, Vol. 46: pp. 78–82, 1979.
- [2] L. Anand. Moderate deformations in extension–torsion of incompressible isotropic elastic materials. *Journal of Mechanics and Physics of Solids*, Vol. 34(3): pp. 293–304, 1986.
- [3] O. T. Bruhns, H. Xiao, and A. Meyers. Hencky's elasticity model with the logarithmic strain measure: a study on poynting effect and stress response in torsion of tubes and rods. *Archives of Mechanics*, Vol. 52(4-5): pp. 489–509, 2000.
- [4] P. Haupt and K. Sedlan. Viscoplasticity of elastomeric materials: experimental facts and constitutive modelling. *Archive of Applied Mechanics*, 71: pp. 89–109, 2001.
- [5] Anne Hoger. The stress conjugate to logarithmic strain. *International Journal of Solids and Structures*, Vol. 23(12): pp. 1645–1656, 1987.
- [6] M. Mooney. A theory of large elastic deformation. *Journal of Applied Physics*, Vol. 11: pp. 582–592, 1940.
- [7] R. W. Ogden. Large deformation isotropic elasticity - on the correlation of theory and experiment for incompressible rubberlike solids. *Proceedings of the Royal Society of London. Series A*, A. 326: pp. 565–584, 1972.
- [8] R. W. Ogden and P. Chadwick. On the deformation of solid and tubular cylinders of incompressible isotropic elastic material. *Journal of Mechanics and Physics of Solids*, Vol. 20: pp. 77–90, 1972.
- [9] J. Plešek, A. Poživilová, and Michal Landa. Application of the logarithmic strain formulation in nonlinear transient dynamic. In Lin Shaopei et al., editor, *CD ROM Proceedings EPMESC'VIII*, Shanghai, 2001. San Lian Publisher.
- [10] J. H. Poynting. On pressure perpendicular to the shear planes in finite pure shears, and on the lengthening of loaded wires when twisted. *Proceedings of the Royal Society of London. Series A*, Vol. 82: pp. 546–559, 1909.
- [11] J. H. Poynting. On the changes in the dimensions of a steel wire when twisted, and on the pressure of distortional waves in steel. *Proceedings of the Royal Society of London. Series A*, Vol. 86: pp. 534–561, 1912.
- [12] A. Poživilová. *Constitutive modelling of hyperelastic materials using the logarithmic description*. PhD thesis, Czech Technical University in Prague, 2002.

- [13] A. Poživilová and F. Fridrich. Experimental verification of logarithmic hyperelastic models. In Jiří Plešek, editor, *Proceedings of Euromech colloquium Formulation and Constitutive Laws for Very Large Strains*, Prague, 2002.
- [14] R. S. Rivlin and D. W. Saunders. Large elastic deformations of isotropic materials VII. experiments on the deformation of rubber. *Philosophical Transactions of the Royal Society of London, Ser. A*, 243: pp. 251–288, 1951.
- [15] K. Sedlan. *Viskoelastisches Materialverhalten von Elastomerwerkstoffen: Experimentelle Untersuchung und Modellbildung*. PhD thesis, Universität Gesamthochschule Kassel, 2000.
- [16] L. R. G. Treloar. Stress-strain data for vulcanised rubber under various types of deformation. *Transactions of the Faraday Society*, Vol. 40: pp. 59–70, 1944.